AEM
Journals.ASM.org

# Carbon Dioxide Fixation by *Metallosphaera yellowstonensis* and Acidothermophilic Iron-Oxidizing Microbial Communities from Yellowstone National Park

**Ryan M. Jennings,[a,b] Laura M. Whitmore,[a,b] James J. Moran,[c] Helen W. Kreuzer,[c] William P. Inskeep[a,b]**

Department of Land Resources and Environmental Sciences, Montana State University, Bozeman, Montana, USA[a]; Thermal Biology Institute, Montana State University, Bozeman, Montana, USA[b]; Pacific Northwest National Laboratories, Richland, Washington, USA[c]

**The fixation of inorganic carbon has been documented in all three domains of life and results in the biosynthesis of diverse organic compounds that support heterotrophic organisms. The primary aim of this study was to assess carbon dioxide fixation in high-temperature Fe(III)-oxide mat communities and in pure cultures of a dominant Fe(II)-oxidizing organism (*Metallosphaera yellowstonensis* strain MK1) originally isolated from these environments. Protein-encoding genes of the complete 3-hydroxypropionate/4-hydroxybutyrate (3-HP/4-HB) carbon dioxide fixation pathway were identified in *M. yellowstonensis* strain MK1. Highly similar *M. yellowstonensis* genes for this pathway were identified in metagenomes of replicate Fe(III)-oxide mats, as were genes for the reductive tricarboxylic acid cycle from *Hydrogenobaculum* spp. (*Aquificales*). Stable-isotope ($^{13}CO_2$) labeling demonstrated $CO_2$ fixation by *M. yellowstonensis* strain MK1 and in *ex situ* assays containing live Fe(III)-oxide microbial mats. The results showed that strain MK1 fixes $CO_2$ with a fractionation factor of ~2.5‰. Analysis of the $^{13}C$ composition of dissolved inorganic C (DIC), dissolved organic C (DOC), landscape C, and microbial mat C showed that mat C is from both DIC and non-DIC sources. An isotopic mixing model showed that biomass C contains a minimum of 42% C of DIC origin, depending on the fraction of landscape C that is present. The significance of DIC as a major carbon source for Fe(III)-oxide mat communities provides a foundation for examining microbial interactions that are dependent on the activity of autotrophic organisms (i.e., *Hydrogenobaculum* and *Metallosphaera* spp.) in simplified natural communities.**

The fixation of inorganic carbon (i.e., carbon dioxide [$CO_2$]) is an important metabolic process in all three domains of life and can initiate trophic cascades that support ecosystem food webs. Photoautotrophs incorporate $CO_2$ by using the Calvin-Benson-Bassham cycle and have long been recognized as significant contributors to the global carbon cycle. The role of archaeal carbon dioxide fixation in microbial communities, however, is not well studied. Until recently, the contribution of chemoautotrophs (specifically *Archaea*) to $CO_2$ fixation has been underappreciated on a global scale, yet the contribution of chemoautotrophic prokaryotes to system productivity is important in numerous habitats. For example, members of the *Thaumarchaeota* (previously referred to as "marine *Crenarchaeota*") represent up to 40% of deep-ocean "bacterioplankton" (1) and have now been implicated as major contributors to global carbon and nitrogen cycling (2–4). Consequently, the discovery of new $CO_2$ fixation pathways and the identification of specific populations that contribute to the fixation of $CO_2$ in natural habitats provide a foundation for understanding how microbial systems contribute to global carbon cycling.

Numerous archaea are capable of $CO_2$ fixation via different mechanisms (5–8). The 3-hydroxypropionate/4-hydroxybutyrate (3-HP/4-HB) and dicarboxylate/4-hydroxybutyrate (DC/4-HB) pathways for $CO_2$ fixation have been identified recently in different members of the *Crenarchaeota* (9, 10). Both cycles regenerate acetyl coenzyme A (CoA) from succinyl-CoA via seven enzyme-catalyzed reactions, including a dehydration reaction (4-hydroxybutyryl-CoA to crotonyl-CoA), which is catalyzed by 4-hydroxybutyryl-CoA dehydratase (4HCD). Consequently, the 4HCD gene (encoding the type 1 4HCD protein) is a marker gene for both pathways. The 3-HP/4-HB pathway has been identified in members of marine and soil *Thaumarchaeota* (1, 11), and the 4HCD gene was found at abundances similar to those of RubisCO, the marker gene for the Calvin-Benson-Bassham cycle, in the Global Ocean Survey (GOS) (9, 12). Therefore, it was suggested that abundant mesophilic autotrophic *Thaumarchaeota* in the open ocean utilize the 3-HP/4-HB cycle (or a variant thereof) to fix substantial quantities of $CO_2$ (9, 10, 13).

Iron oxide microbial mats from acidic (pH ~3) geothermal outflow channels of Yellowstone National Park (YNP) contain chemolithotrophic microorganisms responsible for the oxidation of Fe(II) and the biomineralization of Fe(III)-oxides (14–17). These microbial communities represent a consortium of numerous archaea, including several crenarchaeal populations (orders *Sulfolobales*, *Desulfurococcales*, and *Thermoproteales*) and representatives of the candidate phylum *Geoarchaeota* (18–20), as well as acidophilic bacteria from the order *Aquificales*. *Hydrogenobaculum* spp. are the dominant bacterial population(s) present in high-temperature (i.e., >65°C) acidic Fe mats, and these organisms fix $CO_2$ through a modified version of the reductive tricarboxylic acid

**Received** 18 October 2013 **Accepted** 9 February 2014
**Published ahead of print** 14 February 2014
**Editor:** R. M. Kelly
Address correspondence to Helen W. Kreuzer, Helen.Kreuzer@pnnl.gov, or William P. Inskeep, binskeep@montana.edu.
Supplemental material for this article may be found at http://dx.doi.org/10.1128/AEM.03416-13.

doi:10.1128/AEM.03416-13

(r-TCA) cycle that cleaves citrate via citryl-CoA lyase and citryl-CoA synthetase (21, 22). Mature Fe(III)-oxide mats of a 0.5- to 1-cm thickness contain relatively low levels of *Hydrogenobaculum*-like organisms (2 to 10% of random shotgun sequences). However, these bacteria are important colonizers during the formation of Fe mats (23) and are often found in communities that contain Fe(II)-oxidizing members of the order *Sulfolobales*, such as *Metallosphaera yellowstonensis* (17).

*M. yellowstonensis*-like populations (>98% nucleotide identity to *M. yellowstonensis* strain MK1) represent 10 to 20% of random metagenome sequences from amorphous Fe(III)-oxide mats in YNP, over a temperature range of 60°C to 75°C and a pH range of 2.9 to 3.5 ($n = 8$ metagenome samples) (19, 24, 25). Recent work has shown that *Metallosphaera sedula*, as well as other members of the *Sulfolobales*, fixes $CO_2$ via the 3-HP/4-HB pathway (9, 26), and initial culture experiments with *M. yellowstonensis* in the presence of $CO_2$ and yeast extract (YE) suggested facultative autotrophy (17). However, the fixation of $CO_2$ was neither conclusively demonstrated in pure culture nor shown in environmental samples. Consequently, the objectives of the current study were to (i) identify all 15 candidate genes of the 3-HP/4-HB carbon dioxide fixation pathway in *M. yellowstonensis* strain MK1 and in *de novo* genome assemblies from acidothermophilic Fe(III)-oxide microbial mat communities in YNP, (ii) utilize stable-isotope ($^{13}CO_2$) labeling to obtain direct evidence of $CO_2$ fixation by *M. yellowstonensis* strain MK1 and live Fe(III)-oxide microbial mats, and (iii) determine the extent of $CO_2$ fixation *in situ* by using stable-isotope analysis of different carbon pools within replicate Fe(II)-oxidizing geothermal channels. Results from this study establish that high-temperature Fe(III)-oxide microbial mats contain significant fractions of carbon derived from dissolved inorganic carbon (DIC) and that *M. yellowstonensis*-like organisms present in these systems fix $CO_2$ via the 3-HP/4-HB pathway.

## MATERIALS AND METHODS

**Field sites.** Three different acid-sulfate-chloride geothermal springs in the One Hundred Springs Plain of Norris Geyser Basin, YNP, were sampled for this study, including One Hundred Springs Plain Spring ("OSP Spring") (44°43′58.953″N, 110°42′32.374″W), "Grendel Spring" (44°43′58.0074″N, 110°42′34.4016″W), and "Beowulf Spring" (44°43′53.4″N, 110°42′40.9″W) (these are not official YNP names; thus, coordinates are provided). The source water temperature of all springs ranged from ~80°C to 84°C. Microbial mat samples (3 to 5 g [wet weight]) for the *ex situ* $CO_2$ uptake experiments as well as for direct isotope ratio measurements were excised from the Fe-oxide mat, approximately 2 to 3 m from the source, where the mat temperatures range from 65°C to 72°C. The sampling sites were designated OSP site B (OSP_B), GRN_D, and BE_D. Replicate metagenomes of Fe(III)-oxide mats from OSP Spring and Beowulf Spring were obtained previously (25, 27) and analyzed in this study for all genes important for a complete 3-HP/4-HB cycle. Replicate water samples from 2010 to 2013 were collected and analyzed for both the carbon concentration and isotope content ($\delta^{13}C$) of dissolved (0.2-μm-filtered) and total organic and inorganic carbon (Colorado Plateau Stable Isotope Laboratory, Flagstaff, AZ).

**Genome analysis.** All genes involved in the 3-HP/4-HB cycle, including the key marker 4HCD gene (type I) (9) and the biotin carboxylase subunit of the bifunctional acetyl/propionyl-CoA carboxylase (*accC*) (28), were used as queries to search the genome of *M. yellowstonensis* strain MK1 (National Center for Biotechnology Information BioProject PRJNA64481; taxon identification number 671065) as well as metagenome assemblies from Fe(III)-oxide mats in YNP. Five of these metagenomes were obtained by using 454-Ti sequencing on samples taken on 15 July 2010: Beowulf site D (Genomes OnLine Database [GOLD] sample identification number Gs0000973), Beowulf site E (GOLD sample identification number Gs0000972), One Hundred Springs Plain site B (GOLD sample identification number Gs0000781), One Hundred Springs Plain site C (GOLD sample identification number Gs0000782), and One Hundred Springs Plain site D (GOLD sample identification number Gs0000783). Two of the metagenomes, One Hundred Springs Plain YNP_8 (GOLD sample identification number Gs0000369; sample date, 30 August 2007) and One Hundred Springs Plain YNP_14 (GOLD sample identification number Gs0000371; sample date, 7 November 2007), were sequenced by using Sanger sequencing and were reported in a larger metagenome study of 20 geothermal sites (27). Both *M. yellowstonensis* strain MK1 and *M. yellowstonensis*-like sequences from the One Hundred Springs Plain metagenomes were evaluated for pathway completeness.

**Phylogenetic tree construction.** The phylogenetic relationship of type I 4-hydroxybutyryl-CoA dehydratases and the biotin carboxylase subunit of bifunctional acetyl/propionyl-CoA carboxylases was examined by using MEGA5 (29). Deduced 4HCD proteins were aligned by using the PAM algorithm, and deduced AccC proteins were aligned by using the MUSCLE algorithm. Phylogenetic trees were constructed by using the neighbor-joining method; bootstrap consensus trees and values were inferred from 1,000 replicates. The evolutionary distances were computed by using the Dayhoff matrix-based method.

**Culture media and conditions.** All pure culture experiments and field incubations were performed at 65°C to 70°C in glass medium bottles (total volume, ~710 ml) (part number 219439; Wheaton Science Products) with butyl rubber septum screw caps (part number 240680; Wheaton Science Products). Aqueous medium was synthesized to mimic Fe(III)-oxide spring geochemistry and to provide nutrients sufficient to support up to $10^9$ cells $ml^{-1}$ (see Table S2 in the supplemental material); 300 ml of medium was supplied to each growth vessel. Two and a half grams of ground pyrite was used as a solid-phase ferrous electron donor for each culture. Oxygen headspace was maintained at a partial pressure of >0.6 atm to serve as the electron acceptor. A total of 5 mM inorganic carbon was supplied in the form of $NaHCO_3$ or $NaH^{13}CO_3$ through the bottle septum, after which the pH of the medium was readjusted to ~2.5 with $H_2SO_4$. In some cases, the medium was supplemented with 1% yeast extract as a source of organic carbon.

**Pure-culture $CO_2$ uptake experiments.** *M. yellowstonensis* strain MK1 (17) was grown, as described previously, with $NaH^{13}CO_3$, unlabeled $NaHCO_3$, $NaH^{13}CO_3$, and 1% YE; $NaHCO_3$ and 1% YE; or 1% YE alone for ~10 days to post-log phase (~$10^8$ cells $ml^{-1}$). Culture purity was assessed by using PCR amplification of 16S rRNA with primers for *M. yellowstonensis* and known *Sulfolobales* contaminants (primarily *Sulfolobus islandicus*). Biomass samples were harvested from pure cultures, centrifuged, washed in HCl overnight to remove any potential residual $HCO_3^-$, rinsed three times with deionized $H_2O$, and lyophilized into cell pellets in preparation for isotope ($\delta^{13}C$) analysis via isotope ratio mass spectroscopy.

***Ex situ* incubations.** Approximately 3- to 4-g (wet weight) portions of Fe(III)-oxide microbial mats were excised from the outflow channels of two different Fe(II)-oxidizing geothermal springs (OSP Spring and Grendel Spring), placed into glass medium bottles containing 300 ml synthetic medium with 2.5 g autoclaved ground pyrite mineral, and then sealed with septum-containing lids. The experiment included one sample from OSP Spring, two samples from Grendel Spring that were treated as duplicates, and one sample from each spring that was killed with 0.5 mmol sodium azide. The bottles were purged with pure oxygen for approximately 15 s and brought to a slight positive pressure. Two hundred milliliters of either $^{13}CO_2$ or unlabeled $CO_2$ gas was then added through the septum. Sodium azide-killed controls were injected with $^{13}CO_2$, and all samples were incubated at 65°C to 70°C for 10 days. Positive pressure was maintained in the bottles by injection of additional $O_2$ as needed. After 10

**TABLE 1** Carbon isotope values of *M. yellowstonensis* strain MK1 biomass in growth experiments using labeled versus unlabeled $CO_2$ and 1% yeast extract

| Growth condition | Mean $\delta^{13}C$ value (‰) ($\sigma$) ($n = 3$) | | |
|---|---|---|---|
| | | MK1 biomass | |
| | C source | Culture 1 | Culture 2 |
| 1% YE | −25.1 (0.04) | −24.2 (0.2) | −24.4 (0.2) |
| NA $CO_2$ | −15.9 (0.2) | −19.3 (1.1) | −17.6 (0.8) |
| NA $CO_2$ + 1% YE | | −23.2 (0.1) | −23.2 (0.1) |
| $^{13}CO_2$ | | 71,500 (14,373) | 80,637 (4,166) |
| $^{13}CO_2$ + 1% YE | | 1,677 (37) | 1,540 (153) |

days, biomass was harvested by centrifugation and prepared for isotope analysis, with an HCl wash, deionized $H_2O$ rinse, and lyophilization.

**Isotope ratio mass spectrometry.** Stable carbon isotope ratios ($\delta^{13}C$) were measured by using a Thermo-Finnegan (Bremen, Germany) Delta V Plus isotope ratio mass spectrometer coupled to a Costech Analytical Technologies (Valencia, CA, USA) 4010 Elemental Analyzer and a Zero-Blank autosampler. Approximately 8 to 15 mg of lyophilized iron mat biomass (which contained significant amounts of iron oxide material) or 15 to 20 mg of culture biomass (which contained significant amounts of pyrite) was placed into tin capsules (Costech Analytical Technologies) and analyzed in triplicate. Analytical sample sets included in-house Pacific Northwest National Laboratory (PNNL) glutamic acid standards, which had been calibrated to U.S. Geological Survey (USGS) standard 40 ($\delta^{13}C = -26.39$‰) and USGS standard 41 ($\delta^{13}C = +37.63$‰) glutamic acid isotopic standards. Data were corrected to these standards by using the point-slope method (30). Stable-isotope content is measured as a ratio, $R$ (e.g., $^{13}C/^{12}C$), and reported as a delta ($\delta$) value, where $\delta$ equals $(R_A/R_{Std} - 1) \times 1{,}000$ and $R_A$ and $R_{Std}$ are the isotope ratios of the sample and an internationally recognized standard, respectively. The standard for C isotope ratio analysis is Vienna PeeDee belemnite (VPDB). Special precaution was taken to minimize carryover between analyses. Enriched samples containing large amounts of $^{13}C$ required up to three standard runs to flush the system, as measured by a return to established isotope values. Although excellent precision was obtained for both enriched and natural-abundance (NA) $^{13}C$ samples, enriched samples exhibited poorer analytical precision than natural-abundance samples (standard deviations of sample measurements are reported in Table 1). This was due in part to the fact that enriched samples exceeded the optimum calibration range of the instrument. Also, relatively large sample sizes (up to 20 mg) were required, due to the low carbon contents and large amounts of iron oxide and/or pyrite; this may have influenced combustion efficiency and decreased measurement precision. Despite these caveats, the strong signal from $^{13}C$-enriched cultures and field incubation mixtures provided definitive evidence that inorganic carbon was incorporated into biomass.

**Fractionation factors/mixing models.** The fractionation factor ($\varepsilon$) for *M. yellowstonensis* was determined by using the equation $\varepsilon = 1{,}000 \times \ln(R_{product}/R_{substrate})$, where $R$ is the $^{13}C/^{12}C$ ratio.

The isotopic composition of mat C was predicted by using an isotope mixing model formulated based on $\delta^{13}C$ values of DIC, dissolved organic C (DOC), and landscape C (LC) (measured in this study) and the fractionation factors of *M. yellowstonensis* strain MK1 (this study) and *Hydrogenobaculum*-like organisms (31), which utilize 3-HP/4-HB and r-TCA carbon dioxide fixation pathways, respectively. The measured C isotope content of actual Fe(III)-oxide mat samples may contain contributions from microbial biomass of DIC origin, microbial biomass of DOC (or landscape C) origin, and exogenous landscape C. Given the difficulty in knowing absolute values of all necessary parameters, predicted mat C isotope values were obtained as a function of the ratios of microbial biomass of DIC origin relative to total microbial biomass ($f_{Biomass\text{-}DIC}$, where $f_{Biomass\text{-}DIC} + f_{Biomass\text{-}DOC/LC} = 1$) and the amount of biomass C relative to total mat C ($f_{Biomass\text{-}C}$, where $f_{Biomass\text{-}C} + f_{Nonbiomass\text{-}C} = 1$). Fractionation factors used in the mixing model included a $\varepsilon_{M.\ yellowstonensis}$ value of 2.5‰ (this study) and a $\varepsilon_{Hydrogenobaculum}$ value of 5.5‰ (reported value for *Hydrogenobacter thermophilus* [31]). The assumed fractionation factor for heterotrophic incorporation of organic carbon (DOC or landscape C) was 0‰ (32).

## RESULTS

**Genome and metagenome analysis.** All genes for a complete 3-HP/4-HB cycle were identified in the genome of *M. yellowstonensis* strain MK1 (see Table S1 in the supplemental material), which were similar to those identified in *M. sedula* (9, 33). Moreover, the key marker genes for this pathway (4-hydroxybutyryl-CoA dehydratase [the 4HCD gene] and the biotin subunit of acetyl/propionyl-CoA carboxylase [*accC*]) were found in metagenome sequence assemblies from replicate Fe(III)-oxide mat samples ($n = 6$). The deduced protein sequences obtained from metagenome assemblies are highly similar to and group with the same sequences identified in *M. yellowstonensis* strain MK1 (Fig. 1). Other copies of these marker genes belonging to different *Sulfolobales* were also found in Fe(III)-oxide microbial mats (24), and these populations may also contribute to the fixation of $CO_2$ *in situ*. PCR amplification of the 4HCD gene, *accC*, *accB*, and *pccB*, using primers specific to *M. yellowstonensis* strain MK1, further demonstrated the presence of these genes in both the isolate and Fe(III)-oxide systems (see Fig. S1 in the supplemental material). The metagenome sequence of MK1-like populations present in Fe(III)-oxide mats (~98 to 99% average genome nucleotide identity) contained all genes for a complete 3-HP/4-HB pathway, which were similar to those identified in strain MK1 and *M. sedula* (see Table S1 in the supplemental material). The consistent presence of *M. yellowstonensis*-like 4HCD and *accC* genes in Fe(III)-oxide mat metagenomes suggests that the fixation of $CO_2$ via the 3-HP/4-HB pathway is an important metabolic process conducted by *M. yellowstonensis* populations *in situ* and may result in significant transformation of $CO_2$ to microbial biomass.

**Pure-culture experiments.** Growth experiments using *M. yellowstonensis* strain MK1 in the presence of different C sources provided definitive evidence for the incorporation of $CO_2$ into microbial biomass. The C isotope ratio ($\delta^{13}C$) of *M. yellowstonensis* biomass was −24.3‰ ± 0.2‰ when grown on yeast extract (YE) and ~−18‰ ± 0.5 ‰ when grown on natural-abundance (NA) $CO_2$ (Table 1). When $^{13}CO_2$ was the sole carbon source, $\delta^{13}C$ values of *M. yellowstonensis* biomass were >50,000‰ (Table 1), which demonstrated the incorporation of inorganic carbonate species ($H_2CO_3$ and aqueous $CO_2$ [$CO_2$(aq)] are the dominant species at pH values near 3).

We estimated the $\varepsilon$ value for *M. yellowstonensis* cultures grown on NA $CO_2$, with a measured $^{13}C$ isotope composition of ~−15.9‰ ($R_{substrate} = 0.0114159$) (Table 1). The average value of strain MK1 biomass (−18.45‰; $R_{product} = 0.0114445$) measured in two replicate experiments was used to estimate a value of $\varepsilon$ for *M. yellowstonensis* of ~2.5‰. Although not the primary focus of our study, this $\varepsilon$ value is similar to that observed for *M. sedula* (3.1‰) (31).

When *M. yellowstonensis* was supplied with 1% YE and $CO_2$ simultaneously, $\delta^{13}C$ values showed that carbon constituents from YE were the dominant sources used to build microbial biomass (Table 1). The $^{13}C$ isotope content of *M. yellowstonensis* biomass grown on YE and NA $CO_2$ was slightly higher ($\delta^{13}C$ =

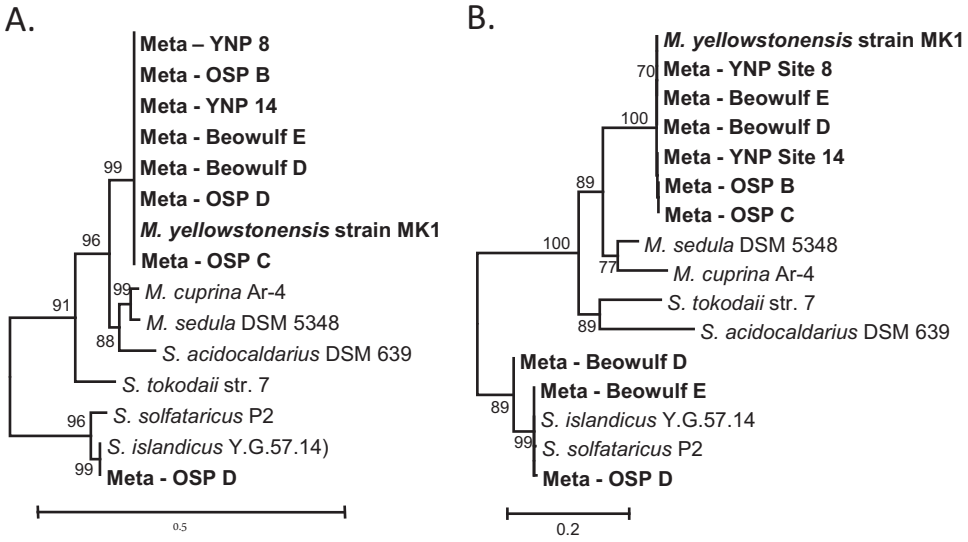


**FIG 1** Phylogenetic trees of key proteins in the 3-HP/4-HB pathway for fixation of carbon dioxide (9). (A) Type I 4-hydroxybutyryl-CoA dehydratase (4HCD); (B) biotin carboxylase subunit of bifunctional acetyl/propionyl-CoA carboxylase (AccC). *Metallosphaera yellowstonensis*-like type I 4HCD and biotin carboxylase sequences were identified in numerous replicate metagenome samples from high-temperature Fe(III)-oxide microbial mats (Beowulf sites D and E, One Hundred Springs Plain sites B and C, YNP_8, and YNP_14).

−23.3‰) than that of biomass grown on YE alone ($\delta^{13}C$ = −24.3‰), which suggested some incorporation of inorganic carbon. The same pattern was observed when strain MK1 was grown on YE plus $^{13}CO_2$. $\delta^{13}C$ values were higher (~1,600‰) than those of biomass grown on YE alone ($\delta^{13}C$ = −24.3‰) but not nearly as high as $^{13}C$ values obtained by using $^{13}CO_2$ alone. Together, these data showed that *M. yellowstonensis* strain MK1 is capable of growth using either $CO_2$ or organic C and that these processes may operate simultaneously (34).

***Ex situ* assays using Fe(III)-oxide mats.** Evidence of a complete 3-HP/4-HB pathway in *M. yellowstonensis* strain MK1 is consistent with the observed incorporation of $CO_2$ using $^{13}CO_2$. The presence of these same genes in metagenome assemblies obtained from Fe(III)-oxide microbial mats (Fig. 1) suggested that this population may fix carbon dioxide *in situ*. To measure the uptake of $CO_2$ in Fe(III)-oxide microbial mats, excised mat samples were incubated *ex situ* with natural-abundance $CO_2$ and $^{13}CO_2$. The uptake of $^{13}CO_2$ into live Fe(III)-oxide mats was observed in two different geothermal communities studied (Table 2). Small increases in the $^{13}C$ content of killed controls were also observed, but these values were considerably lower than those observed with live mats and may be due to abiotic exchange between $^{13}CO_2$ and solid phases and/or incomplete sterility achieved by using sodium azide.

**Carbon isotope composition of iron geothermal systems.** The $^{13}C$ compositions ($\delta^{13}C$) of dissolved inorganic carbon (DIC), dissolved organic carbon (DOC), Fe(III)-oxide mat carbon, and various landscape carbon samples were analyzed to evaluate the likely contributions of these potential C sources to microorganisms within native Fe mat communities (Table 3). The $^{13}C$ isotope contents of landscape components such as leaves, soil, and animal dung from around the spring sites were characteristic of $C_3$

**TABLE 2** Carbon isotope composition of microbial mat samples incubated after *ex situ* experiments to detect $CO_2$ uptake in Fe(III)-oxide microbial mat communities from Norris Geyser Basin, YNP, October 2011

| Treatment | Sample[a] | $\delta^{13}C$ value (‰) (σ) ($n$ = 3) |
|---|---|---|
| $CO_2$ NA, live mat | OSP_B | −16.1 (0.1) |
| $CO_2$ NA, live mat | GRN_D | −13.8 (0.2) |
| $^{13}CO_2$, live mat | OSP_B, assay 1 | 1,278 (61) |
| $^{13}CO_2$, live mat | GRN_D, assay 1 | 1,267 (95) |
| $^{13}CO_2$, live mat | GRN_D, assay 2 | 1,458 (54) |
| $^{13}CO_2$, killed | OSP_B | 27.3 (2.0) |
| $^{13}CO_2$, killed | GRN_D | 46.9 (3.7) |

[a] OSP_B, One Hundred Springs Plain Spring site B; GRN_D, Grendel Spring site D.

**TABLE 3** Carbon isotope ratios of dissolved inorganic carbon, dissolved organic C, and total C present in Fe(III)-oxide microbial mats collected from Norris Geyser Basin, YNP, 2011 to 2013

| Carbon pool | Sample[a] | $\delta^{13}C$ value (‰) (σ) (no. of samples) | Concn (mg $kg^{-1}$) (σ) (no. of samples)[b] |
|---|---|---|---|
| DIC | OSP_B | −5.1 (0.8) (3) | 1.5 (0.8) (3) |
| | BE_D | −3.2 (0.2) (4) | 2.0 (1.9) (4) |
| | GRN_D | −0.5 (2.6) (3) | 0.6 (0.1) (3) |
| DOC | OSP_B | −21.0 (1.6) (3) | 0.8 (0.5) (3) |
| | BE_D | −22.3 (1.0) (5) | 0.8 (0.7) (4) |
| | GRN_D | −23.0 (2.1) (4) | 0.6 (0.2) (3) |
| Microbial mat[c] | OSP_B | −15.0 (1.8) (3) | 10,200 |
| | BE_D | −16.4 (1.1) (8) | 11,500 |
| | GRN_D | −16.5 (0.9) (3) | 7,600 |

[a] OSP_B, One Hundred Springs Plain Spring site B; BE_D, Beowulf Spring site D; GRN_D, Grendel Spring site D.
[b] Expressed as mg per liter for DIC and DOC and mg per kg (dry weight) for microbial mat C.
[c] The total C level was determined on aggregate mat samples from each site during this time frame ($n$ = 1). The range of 0.8 to 1.5% total C agrees favorably with values observed in previous studies (16).

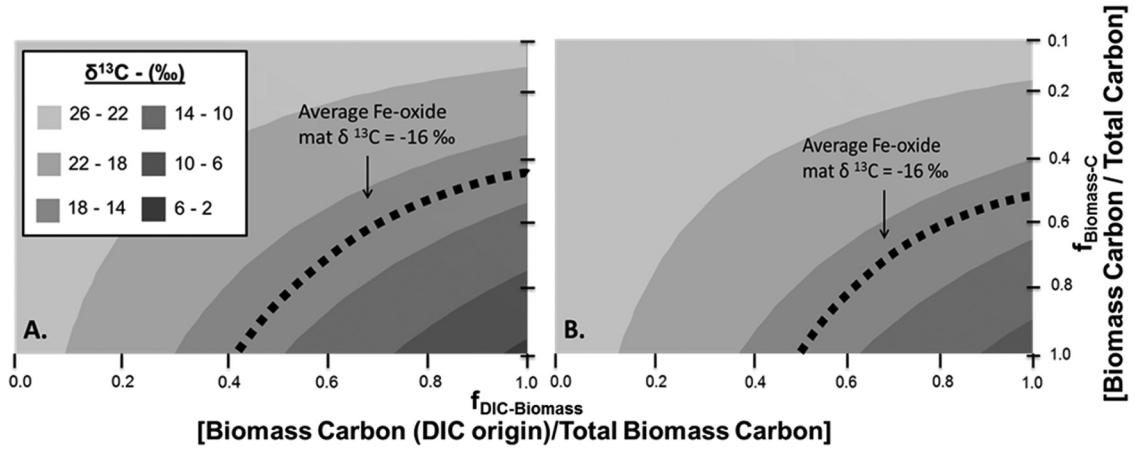


**FIG 2** Predicted $\delta^{13}C$ content of Fe(III)-oxide microbial mats as a function of the fraction of microbial biomass originating from dissolved inorganic C (DIC) relative to total biomass C (*x* axis) and the fraction of biomass C relative to total Fe mat C (*y* axis). Fixation of $CO_2$ may occur via the 3-HP/4-HB pathway (i.e., *M. yellowstonensis*) (A) or the r-TCA pathway (i.e., *Hydrogenobaculum* sp.) (B). The isotope mixing model was based on the measured isotope composition of DIC, DOC, and landscape C sources and specific fractionation factors for the conversion of $CO_2$ to microbial biomass (see Materials and Methods). The average observed $^{13}C$ content ($\delta^{13}C$, ~−16‰) (dotted line) from replicate Fe(III)-oxide microbial mats shows that at least 42 to 50% of the biomass carbon has a DIC origin.

photosynthesis ($\delta^{13}C$, ~−26‰) and are consistent with predictions based on the high latitude and elevation of Yellowstone National Park (35, 36). The $^{13}C$ composition of DOC averaged −22.2‰ ($\sigma$ = 1.6‰) across the three geothermal systems studied and was slightly higher (Table 3) than that of landscape C. Conversely, the $^{13}C$ content of the DIC fraction ranged from −5.1‰ to 0.49‰ across the three springs (Table 3). Relative to either DOC or landscape C, the DIC fraction has significantly high $^{13}C$ content and provides a basis for interpreting the isotopic composition of mat biomass. The mean $\delta^{13}C$ of three Fe(III)-oxide microbial mats ($n$ = 14) was −16.1‰ ($\sigma$= 1.3‰) and ranged from −16.5‰ in samples from Grendel Spring (GRN_D) to −15.0‰ in samples from One Hundred Springs Plain (OSP_B) (Table 3). These values fall between the $^{13}C$ compositions of end-member DIC and DOC (or landscape C) and show that Fe(III)-oxide microbial mats contain carbon of both organic and inorganic origins and that DIC makes a significant contribution to mat carbon.

## DISCUSSION

The incorporation of $^{13}CO_2$ into live microbial Fe(III)-oxide mats demonstrated that organisms within these communities are capable of $CO_2$ fixation and that this is an important process *in situ*. We also showed that pure cultures of *M. yellowstonensis* strain MK1, a significant community member in these Fe(III)-oxide microbial mats, grew using $CO_2$ as the sole C source in the absence of yeast extract (fractionation factor [ε] = 2.5‰). High-temperature acidic Fe(III)-oxide mat communities are typically composed of 5 to 7 major phylotypes, including *M. yellowstonensis* and *Hydrogenobaculum*-like populations, which represent 10 to 20% and 2 to 10% of the community, respectively, based on random sequence reads of mature Fe mat metagenomes (19, 24, 25). Other archaea present in these communities include members of two novel archaeal groups, the *Thaumarchaeota* and the *Euryarchaeota* (*Thermoplasmatales*-like), as well as other crenarchaea within the orders *Thermoproteales* and *Desulfurococcales* (19, 24, 25). However, sequence assemblies corresponding to these populations do not contain evidence of marker genes for known $CO_2$ fixation pathways and appear to be primarily heterotrophic (18, 19, 24, 25, 37, 41). Despite the diversity of archaea in these Fe(II)-oxidizing communities, the only known $CO_2$ fixation pathways found in metagenome sequence analyses included the 3-HP/4-HB pathway (contributed by *M. yellowstonensis*-like and other *Sulfolobales* populations) and the r-TCA cycle (contributed by *Hydrogenobaculum*-like populations). Thus, our working hypothesis is that *M. yellowstonensis*- and *Hydrogenobaculum*-like populations are the primary members of mature Fe(III)-oxide mat communities that contribute to the fixation of $CO_2$ into mat biomass.

Isotopic analysis of the major carbon pools (DIC, DOC, landscape carbon, and Fe mat carbon) from three geothermal sites showed that mat carbon exhibits an isotopic composition of ~−16.1‰ ($\sigma$ = 1.3‰) (Table 3), which is between the $^{13}C$ contents of DIC and DOC (or landscape C) end members (Table 3). Therefore, the $^{13}C$ values of mat C can be explained as a mixture of biomass carbon originating from DIC (i.e., autotrophy), DOC, and/or landscape C (heterotrophy) and, simultaneously, as a possible mixture of biomass carbon and exogenous landscape C from foreign sources (e.g., plant material, insects, landscape detritus, and eukaryal biomass), although any visible macroscopic debris was avoided during sampling. An isotope mixing model (Fig. 2) was developed to predict the isotopic composition of C present in Fe(III)-oxide microbial mats as a function of (i) the fraction of biomass C of DIC origin ($f_{DIC\text{-}Biomass}$) and (ii) the fraction of biomass C relative to total mat C ($f_{Biomass\text{-}C}$) (Fig. 2). Given the similarity of $\delta^{13}C$ values for DOC and landscape C (−22 to −26‰), it is not possible to distinguish heterotrophic biomass generated from either of these carbon sources. Carbon isotope fractionation factors for heterotrophic metabolism are near 0‰ (32); consequently, the $^{13}C$ content of biomass C generated from either DOC or landscape C will also range from ~−22 to −26‰.

Two different isotopic mixing models were evaluated based on autotrophic contributions from either the 3-HP/4-HB cycle (*M. yellowstonensis*) or the r-TCA cycle (*Hydrogenobaculum* spp.) (Fig. 2). Fractionation factors for the conversion of DIC to microbial biomass were obtained either in this study (*M. yellowstonensis*, ε =

2.5‰) or from literature sources (*Hydrogenobaculum*, $\varepsilon = 5.5‰$ [31]). Estimates of the autotrophic contribution to biomass C ($f_{DIC\text{-}Biomass}$) (*x* axis in Fig. 2) are relatively insensitive to the range of fractionation factors available for the conversion of $CO_2$ to microbial biomass, due to the large differences in $\delta^{13}$C-DIC versus $\delta^{13}$C-DOC values. Although the fixation of $CO_2$ can also be weighted based on the relative ratio of the amount of *Metallosphaera* to the amount of *Hydrogenobaculum* observed in random metagenome sequencing (~4:1), the model solution falls between those shown for the two cases based on either organism alone (Fig. 2A and B).

The average observed Fe(III)-oxide mat $\delta^{13}$C value of −16.1‰ (Fig. 2, dotted line) is constrained by a unique set of the fraction of DIC in microbial biomass ($f_{DIC\text{-}Biomass}$) versus the fraction of microbial biomass C relative to total Fe mat C ($f_{Biomass\text{-}C}$). The observed $^{13}$C isotopic composition can be explained only when the $f_{DIC\text{-}Biomass}$ ranges from about 0.42 to >0.99, depending on the dilution of microbial biomass C with nonmicrobial C from landscape sources (Fig. 2). Greater contributions of nonmicrobial landscape C to Fe mat C result in correspondingly higher estimates of $f_{DIC\text{-}Biomass}$. In the simplest case, where the Fe mat contains no exogenous landscape C ($f_{Biomass\text{-}C} = 1$), the mat $^{13}$C content is explained by $f_{DIC\text{-}Biomass}$ values of ~0.42 to 0.50, depending on whether $CO_2$ is fractionated via the 3-HP/4-HB or r-TCA pathway (Fig. 2A and B). Interestingly, this is greater than, but agrees favorably with, the absolute abundance of the two primary DIC-fixing populations identified previously by using metagenome sequencing (the combined abundance of *Metallosphaera* and *Hydrogenobaculum* populations has ranged from 20 to 35% of the community). Growth and turnover rates of all populations present in these communities may not be equal, and less abundant, faster-growing autotrophic populations (relative to heterotrophic populations) could also influence observed mat $\delta^{13}$C values. It is possible that heterotrophic populations present in these communities utilize biomass or metabolites produced only from autotrophs (i.e., classical primary production), which would correspond to $f_{DIC\text{-}Biomass}$ values close to 1. In this scenario, nearly 50 to 60% of the total mat C would have to be nonmicrobial C from landscape sources (Fig. 2).

The total C content of Fe-oxide microbial mats is ~1%, and only a fraction of this carbon (as much as 10%) can be accounted for in estimates of live-cell counts (~$10^9$ cells $g^{-1}$) (18, 24, 25, 38), although the filamentous nature of specific phylotypes makes accurate cell counting difficult. The remaining carbon present in Fe(III)-oxide mats is comprised of dead microbial biomass generated *in situ* and/or exogenous landscape C. The sorption of DOC by Fe(III)-oxides may also contribute to mat C (39); however, the available surface sites of the amorphous Fe(III)-oxide phases present in these systems are nearly saturated with arsenate as bidentate surface complexes (16). Consequently, future efforts should focus on evaluation of live versus dead biomass C, other solid phases of exogenous C, and a more detailed characterization of components comprising the DOC fraction.

Results from this study have important implications for possible microbial interactions occurring among community members in thermoacidic Fe(II)-oxidizing microbial communities. The isotopic composition of total mat C in all three springs showed that $CO_2$ fixation is an important process *in situ*, which provides a source of organic carbon and numerous possible substrates for heterotrophic community members. These data are consistent with the hypothesis that *M. yellowstonensis* and *Hydrogenobaculum* spp. serve founding roles in the development of Fe(III)-oxide mats and community succession (23, 40). Now that the incorporation of inorganic carbon by members of these communities has been firmly established, more detailed trophic cascades and metabolite interactions may be resolvable by using stable-isotope probing coupled with metabolomic and/or proteomic analyses. Colonization by one or both of the predominant $CO_2$-fixing populations (*Metallosphaera* and *Hydrogenobaculum*) may be a necessary condition for establishing acidothermophilic Fe(III)-oxide mat communities, which also support significant heterotrophic diversity.

## ACKNOWLEDGMENTS

We acknowledge and appreciate funding from the National Science Foundation Integrative Graduate and Education Training (IGERT) Program (DGE 0654336) for support to R.M.J.; the Howard Hughes Undergraduate Fellowship Program for support to L.M.W.; the Department of Energy Genome Science Program, Microbial Interactions Foundational Science Focus Area (Pacific Northwest National Laboratory subcontract 112443 to Montana State University); and the Montana Agricultural Experiment Station (project 911300 to W.P.I.).

We appreciate research permits (permit no. YELL-5568, 2007-2010) managed by C. Hendrix and S. Gunther (Center for Resources, YNP) and discussion with J. Beam, Z. Jay, M. Kozubal, and M. Romine.

## REFERENCES

1. **Karner MB, DeLong EF, Karl DM.** 2001. Archaeal dominance in the mesopelagic zone of the Pacific Ocean. Nature **409:**507–510. http://dx.doi.org/10.1038/35054051.
2. **Pearson A, McNichol AP, Benitez-Nelson BC, Hayes JM, Eglinton TI.** 2001. Origins of lipid biomarkers in Santa Monica Basin surface sediment: a case study using compound-specific $\delta^{14}$C analysis. Geochim. Cosmochim. Acta **65:**3123–3137. http://dx.doi.org/10.1016/S0016-7037(01)00657-3.
3. **Könneke M, Bernhard AE, De la Torre JR, Walker CB, Waterbury JB, Stahl DA.** 2005. Isolation of an autotrophic ammonia-oxidizing marine archaeon. Nature **437:**543–546. http://dx.doi.org/10.1038/nature03911.
4. **Tully BJ, Nelson WC, Heidelberg JF.** 2012. Metagenomic analysis of a complex marine planktonic thaumarchaeal community from the Gulf of Maine. Environ. Microbiol. **14:**254–267. http://dx.doi.org/10.1111/j.1462-2920.2011.02628.x.
5. **Huber H, Huber R, Stetter KO.** 2006. Thermoproteales, p 10–22. *In* Dworkin M, Falkow S, Rosenberg E, Schleifer K-H, Stackebrandt E (ed), The prokaryotes. Springer, New York, NY.
6. **Huber H, Prangishvili D.** 2006. Sulfolobales, p 23–51. *In* Dworkin M, Falkow S, Rosenberg E, Schleifer K-H, Stackebrandt E (ed), The prokaryotes. Springer, New York, NY.
7. **Huber H, Stetter KO.** 2006. Desulfurococcales, p 52–68. *In* Dworkin M, Falkow S, Rosenberg E, Schleifer K-H, Stackebrandt E (ed), The prokaryotes. Springer, New York, NY.
8. **Hügler M, Huber H, Stetter KO, Fuchs G.** 2003. Autotrophic $CO_2$ fixation pathways in archaea (Crenarchaeota). Arch. Microbiol. **179:**160–173. http://dx.doi.org/10.1007/s00203-002-0512-5.
9. **Berg IA, Kockelkorn D, Buckel W, Fuchs G.** 2007. A 3-hydroxypropionate/4-hydroxybutyrate autotrophic carbon dioxide assimilation pathway in archaea. Science **318:**1782–1786. http://dx.doi.org/10.1126/science.1149976.
10. **Huber H, Gallenberger M, Jahn U, Eylert E, Berg IA, Kockelkorn D, Eisenreich W, Fuchs G.** 2008. A dicarboxylate/4-hydroxybutyrate autotrophic carbon assimilation cycle in the hyperthermophilic archaeum *Ignicoccus hospitalis*. Proc. Natl. Acad. Sci. U. S. A. **105:**7851–7856. http://dx.doi.org/10.1073/pnas.0801043105.
11. **Zhang L-M, Offre PR, He J-Z, Verhamme DT, Nicol GW, Prosser JI.** 2010. Autotrophic ammonia oxidation by soil Thaumarchaea. Proc. Natl. Acad. Sci. U. S. A. **107:**17240–17245. http://dx.doi.org/10.1073/pnas.1004947107.
12. **Rusch DB, Halpern AL, Sutton G, Heidelberg KB, Williamson S,**

**Yooseph S, Wu D, Eisen JA, Hoffman JM, Remington K, Beeson K, Tran B, Smith H, Baden-Tillson H, Stewart C, Thorpe J, Freeman J, Andrews-Pfannkoch C, Venter JE, Li K, Kravitz S, Heidelberg JF, Utterback T, Rogers Y-H, Falcón LI, Souza V, Bonilla-Rosso G, Eguiarte LE, Karl DM, Sathyendranath S, Platt T, Bermingham E, Gallardo V, Tamayo-Castillo G, Ferrari MR, Strausberg RL, Nealson K, Friedman R, Frazier M, Venter JC.** 2007. The Sorcerer II global ocean sampling expedition: northwest Atlantic through eastern tropical Pacific. PLoS Biol. **5:**e77. http://dx.doi.org/10.1371/journal.pbio.0050077.

13. **Ramos-Vera WH, Berg IA, Fuchs G.** 2009. Autotrophic carbon dioxide assimilation in Thermoproteales revisited. J. Bacteriol. **191:**4286–4297. http://dx.doi.org/10.1128/JB.00145-09.
14. **Konhauser KO.** 1998. Diversity of bacterial iron mineralization. Earth Sci. Rev. **43:**91–121. http://dx.doi.org/10.1016/S0012-8252(97)00036-6.
15. **Nordstrom DK, Southam G.** 1997. Geomicrobiology of sulfide mineral oxidation. Rev. Miner. Geochem. **35:**361–390.
16. **Inskeep WP, Macur RE, Harrison G, Bostick BC, Fendorf S.** 2004. Biomineralization of As(V)-hydrous ferric oxyhydroxide in microbial mats of an acid-sulfate-chloride geothermal spring, Yellowstone National Park. Geochim. Cosmochim. Acta **68:**3141–3155. http://dx.doi.org/10.1016/j.gca.2003.09.020.
17. **Kozubal MA, Macur RE, Korf S, Taylor WP, Ackerman GG, Nagy A, Inskeep WP.** 2008. Isolation and distribution of a novel iron-oxidizing crenarchaeon from acidic geothermal springs in Yellowstone National Park. Appl. Environ. Microbiol. **74:**942–949. http://dx.doi.org/10.1128/AEM.01200-07.
18. **Kozubal MA, Romine M, Jennings RM, Jay ZJ, Tringe SG, Rusch DB, Beam JP, McCue LA, Inskeep WP.** 2013. Geoarchaeota: a new candidate phylum in the Archaea from high-temperature acidic iron mats in Yellowstone National Park. ISME J. **7:**622–634. http://dx.doi.org/10.1038/ismej.2012.132.
19. **Inskeep WP, Jay ZJ, Herrgard MJ, Kozubal MA, Rusch DB, Tringe SG, Macur RE, Jennings RM, Boyd ES, Spear JR, Roberto FF.** 2013. Phylogenetic and functional analysis of metagenome sequence from high-temperature archaeal habitats demonstrate linkages between metabolic potential and geochemistry. Front. Microbiol. **4:**95. http://dx.doi.org/10.3389/fmicb.2013.00095.
20. **Takacs-Vesbach C, Inskeep WP, Jay ZJ, Herrgard MJ, Rusch DB, Tringe SG, Kozubal MA, Hamamura N, Macur RE, Fouke BW, Reysenbach A-L, McDermott TR, Jennings RM, Hengartner NW, Xie G.** 2013. Metagenome sequence analysis of filamentous microbial communities obtained from geochemically distinct geothermal channels reveals specialization of three Aquificales lineages. Front. Microbiol. **4:**84. http://dx.doi.org/10.3389/fmicb.2013.00084.
21. **Boyd ES, Leavitt WD, Geesey GG.** 2009. $CO_2$ uptake and fixation by a thermoacidophilic microbial community attached to precipitated sulfur in a geothermal spring. Appl. Environ. Microbiol. **75:**4289–4296. http://dx.doi.org/10.1128/AEM.02751-08.
22. **Hügler M, Huber H, Molyneaux SJ, Vertriani C, Sievert SM.** 2007. Autotrophic $CO_2$ fixation via the reductive tricarboxylic acid cycle in different lineages within the phylum Aquificae: evidence for two ways of citrate cleavage. Environ. Microbiol. **9:**81–92. http://dx.doi.org/10.1111/j.1462-2920.2006.01118.x.
23. **Macur RE, Langner HW, Kocar BD, Inskeep WP.** 2004. Linking geochemical processes with microbial community analysis: successional dynamics in an arsenic-rich, acid-sulphate-chloride geothermal spring. Geobiology **2:**163–177. http://dx.doi.org/10.1111/j.1472-4677.2004.00032.x.
24. **Kozubal MA, Macur RE, Jay ZJ, Beam JP, Malfatti SA, Tringe SG, Kocar BD, Borch T, Inskeep WP.** 2012. Microbial iron cycling in acidic geothermal springs of Yellowstone National Park: integrating molecular surveys, geochemical processes, and isolation of novel Fe-active microorganisms. Front. Microbiol. **3:**109. http://dx.doi.org/10.3389/fmicb.2012.00109.
25. **Inskeep WP, Rusch DB, Jay ZJ, Herrgard MJ, Kozubal MA, Richardson TH, Macur RE, Hamamura N, Jennings RM, Fouke BW, Reysenbach A-L, Roberto F, Young M, Schwartz A, Boyd ES, Badger JH, Mathur EJ, Ortmann AC, Bateson M, Geesey G, Frazier M.** 2010. Metagenomes from high-temperature chemotrophic systems reveal geochemical controls on microbial community structure and function. PLoS One **5:**e9773. http://dx.doi.org/10.1371/journal.pone.0009773.
26. **Berg IA, Kockelkorn D, Ramos-Vera WH, Say RF, Zarzycki J, Hügler M, Birgit E, Alber BE, Fuchs G.** 2010. Autotrophic carbon fixation in archaea. Nat. Rev. Microbiol. **8:**447–460. http://dx.doi.org/10.1038/nrmicro2365.
27. **Inskeep WP, Jay ZJ, Tringe SG, Herrgård MJ, Rusch DB, YNP Metagenome Project Steering Committee and Working Group Members.** 2013. The YNP metagenome project: environmental parameters responsible for microbial distribution in the Yellowstone geothermal ecosystem. Front. Microbiol. **4:**67. http://dx.doi.org/10.3389/fmicb.2013.00067.
28. **Hügler M, Krieger RS, Jahn M, Fuchs G.** 2003. Characterization of acetyl-CoA/propionyl-CoA carboxylase in *Metallosphaera sedula*: carboxylating enzyme in the 3-hydroxypropionate cycle for autotrophic carbon fixation. Eur. J. Biochem. **270:**736–744. http://dx.doi.org/10.1046/j.1432-1033.2003.03434.x.
29. **Tamura K, Peterson D, Peterson N, Stecher G, Nei M, Kumar S.** 2011. MEGA5: molecular evolutionary genetics analysis using maximum likelihood, evolutionary distance, and maximum parsimony methods. Mol. Biol. Evol. **28:**2731–2739. http://dx.doi.org/10.1093/molbev/msr121.
30. **Coplen TB, Brand WA, Gehre M, Gröning M, Meijer HAJ, Toman B, Verkouteren RM.** 2006. New guidelines for $\delta^{13}C$ measurements. Anal. Chem. **78:**2439–2441. http://dx.doi.org/10.1021/ac052027c.
31. **House CH, Schopf JW, Stetter KO.** 2003. Carbon isotopic fractionation by archaeans and other thermophilic prokaryotes. Org. Geochem. **34:**345–356. http://dx.doi.org/10.1016/S0146-6380(02)00237-1.
32. **Boschker HTS, Middelburg JJ.** 2002. Stable isotopes and biomarkers in microbial ecology. FEMS Microbiol. Ecol. **40:**85–95. http://dx.doi.org/10.1111/j.1574-6941.2002.tb00940.x.
33. **Hawkins AS, Han Y, Bennett RK, Adams MWW, Kelly RM.** 2013. Role of 4-hydroxybutyrate-CoA synthetase in the $CO_2$ fixation cycle in thermoacidophilic archaea. J. Biol. Chem. **228:**4012–4022. http://dx.doi.org/10.1074/jbc.M112.413195.
34. **Auernik KS, Kelly RM.** 2010. Physiological versatility of the extremely thermoacidophilic archaeon *Metallosphaera sedula* supported by transcriptomic analysis of heterotrophic, autotrophic, and mixotrophic growth. Appl. Environ. Microbiol. **76:**931–935. http://dx.doi.org/10.1128/AEM.01336-09.
35. **Ehleringer JR, Monson RK.** 1993. Evolutionary and ecological aspects of photosynthetic pathway variation. Annu. Rev. Ecol. Syst. **24:**411–439. http://dx.doi.org/10.1146/annurev.es.24.110193.002211.
36. **Stowe LG, Teeri JA.** 1978. The geographic distribution of C4 species of the Dicotyledonae in relation to climate. Am. Nat. **112:**609–623. http://dx.doi.org/10.1086/283301.
37. **Beam JP, Jay ZJ, Kozubal MA, Inskeep WP.** 2013. Niche specialization of novel Thaumarchaeota to oxic and hypoxic acidic geothermal springs of Yellowstone National Park. ISME J. http://dx.doi.org/10.1038/ismej.2013.193.
38. **Bernstein HC, Beam JP, Kozubal MA, Carlson RP, Inskeep WP.** 2013. In situ analysis of oxygen consumption and diffusive transport in high-temperature acidic iron-oxide microbial mats. Environ. Microbiol. **15:**2360–2370. http://dx.doi.org/10.1111/1462-2920.12109.
39. **Ali MA, Dzombak DA.** 1996. Competitive sorption of simple organic acids and sulfate on goethite. Environ. Sci. Technol. **30:**1061–1071. http://dx.doi.org/10.1021/es940723g.
40. **Beam JP, Jay ZJ, Kozubal MA, Inskeep WP.** 2011. Distribution and ecology of thaumarchaea in geothermal environments, abstr PA-009. Abstr. 11th Int. Conf. Thermophiles Res., Big Sky, MT.
41. **Jay ZJ, Rusch DB, Tringe SG, Bailey C, Jennings RM, Inskeep WP.** 2014. Predominant *Acidilobus*-like populations from geothermal environments in Yellowstone National Park exhibit similar metabolic potential in different hypoxic microbial communities. Appl. Environ. Microbiol. **80:**294–305. http://dx.doi.org/10.1128/AEM.02860-13.